Supporting information

Gold nanoparticle as an outstanding catalyst for the hydrogen evolution reaction

Tien D. Tran,[a] Mai T.T. Nguyen,[b*] Hoang V. Le,[a] Duc N. Ngoc,[a] Quang Duc Truong,[c] Phong D. Tran[a,d*]

[a]*Department of Advanced Materials Science and Nanotechnology, University of Science and Technology of Hanoi, Vietnam Academy of Science and Technology, 18 Hoang Quoc Viet, Ha Noi, Viet Nam. Email: tran-dinh.phong@usth.edu.vn*

[b]*School of Chemical Engineering, Hanoi University of Science and Technology, 1 Dai Co Viet road, Ha Noi, Viet Nam. Email: nguyenthituyetmai87@gmail.com*

[c]*Institute of Multidisciplinary Research for Advanced Materials, Tohoku University, Sendai 980-8577, Japan*

[d]*Department of Chemistry, College of Natural Sciences, Hanyang University, Seoul 04763, Republic of Korea. Email: trandp@hanyang.ac.kr*

Chemicals

Gold chloride trihydrate ($HAuCl_4.3H_2O$, 99%), terpyridine ($C_{15}H_{11}N_3$, 98%), bipyridine ($C_{10}H_8N_2$, ≥98%), L-cysteine ($C_3H_7NO_2S$, ≥97%), methanesulfonic acid (CH_3SO_3H, ≥97%) and trisodium citrate dehydrate ($Na_3C_6H_5O_7.2H_2O$, 99%) were purchased from Sigma-Aldrich. Hexadecyltrimethyl ammonium bromide ($C_{19}H_{42}BrN$, ≥97%) were purchased from Merck. All these chemicals were used as received without any purification. Deionized water was used in all the preparations.

Preparation of colloidal gold nanoparticles (Au-NPs-13nm)

Colloidal gold nanoparticles, having size of 13 nm, were prepared following the method described previously by Turkevich group using trisodium citrate as both reducing agent and surfactant which stabilizes the Au-NPs. 10 mL of $HAuCl_4$ aqueous solution (2.10^{-3} M) was heated to 70°C and 10 mL of aqueous trisodium citrate (8.10^{-3} M) was added to the heated solution with good mechanical stirring. After about a minute a very faint greyish-blue tone appeared gradually darkening over a period of about 5 min. After 45 min, the final color was wine red, which indicated the formation of Au-NPs. The obtained liquid was cooled to room temperature. The final product was isolated by two cycles of centrifugation at 13 000 rpm for 10 min followed by removal of the supernatant.

Preparation solutions of different surfactants

10 mM solution of different surfactant (*e.g.* bipyridine and terpyridine in dichloromethane and MAS, CTAB, L-cysteine in water) was prepared. To these solutions, a steady 350µg-Au-NPs-13nm/FTO electrode was immersed for 30 min, followed by drying in air.

Instrumentation

The absorption spectra were recorded using a SHIMADZU UV-1280 spectrometer in the 200 to 900 nm range. Scanning electron microscope (SEM) images of the nanostructures were recorded on a Hitachi S4800 microscope. TEM characterizations were performed using a Jeol 100-CX II microscope operating at 100 kV. X-ray diffraction (XRD) spectra of gold nanoparticles were recorded on a Empyrean Diffractometer-Panalytical Monochromatic Cu-Kα radiation. The Fourier transform-infrared (FT-IR) spectra were obtained by a Thermo Nicolet iS-10 spectrometer equipped with attenuated total reflection. Infrared spectra were recorded in the range of 4000–500 cm^{-1} by 64 scans per spectrum at 4 cm^{-1} resolution.

X-ray Photoelectron Spectroscopic (XPS) analysis was conducted using an ESCALAB 220i-XL X-ray photoelectron spectroscopy (XPS) system equipped with a hemispherical analyzer. The background pressure in the analysis chamber was in the 10^{-10} Torr range. The analyzer was calibrated with gold, silver, and copper polycrystalline standard samples by setting the Au $4f_{7/2}$, Ag $3d_{5/2}$ and Cu $2p_{3/2}$ peaks at binding energies of 83.98±0.02, 368.26±0.02, and 932.67±0.02 eV. The survey and high-energy resolution scans were recorded with pass energies of 150 and 20 eV, respectively.

H_2-evolving catalytic activity assay

All electrochemical measurements were conducted on Metrohm Autolab PG302N potentiostat.

A working electrode was made by drop casting 50 μL, 100 μL, 150 μL, 200 μL, 250 μL of the catalyst (prepared Au-NPs solutions) to cover a fixed area on fluorine-doped tin oxide coated glass slide (FTO glass) (a circle of 6 mm diameter). Before this step, FTO glass was carefully washed

in ultrasonic bath with acetone, ethanol and then double distilled water. The reference was an Ag/AgCl/KCl electrode. The counter was a glassy carbon rod electrode. The electrolyte was a O_2-free pH 0 H_2SO_4 or a phosphate buffer solution. The potential scan rate was 2mV/s. The potential range to scan is between -0.25V and 0.2V (*vs.* RHE).

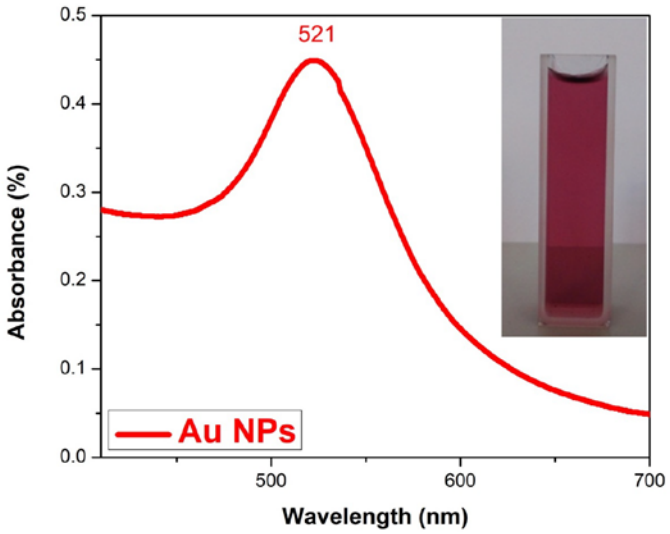

Figure S1. Absorption spectrum and digital image (insert) of a synthesized Au-NPs-13nm solution.

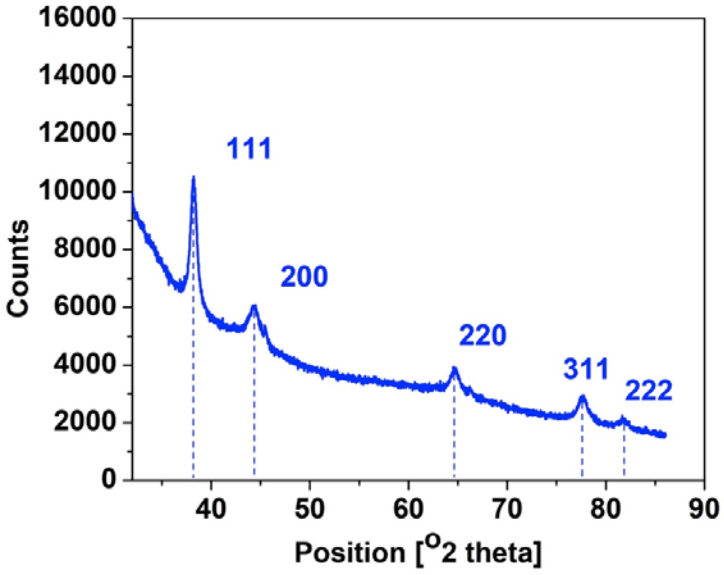

Figure S2. XRD pattern of synthesized Au-NPs-13nm.

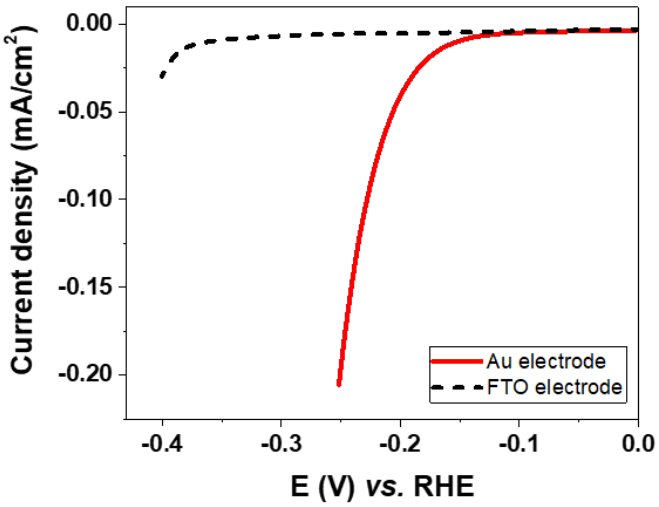

Figure S3. Steady I-V curves recorded on a clean FTO (black dashed curve) and a clean Au disk (red curve) electrodes. Electrolyte was a O_2-free pH 0 H_2SO_4 solution. Potential scan rate was 2 mV/s.

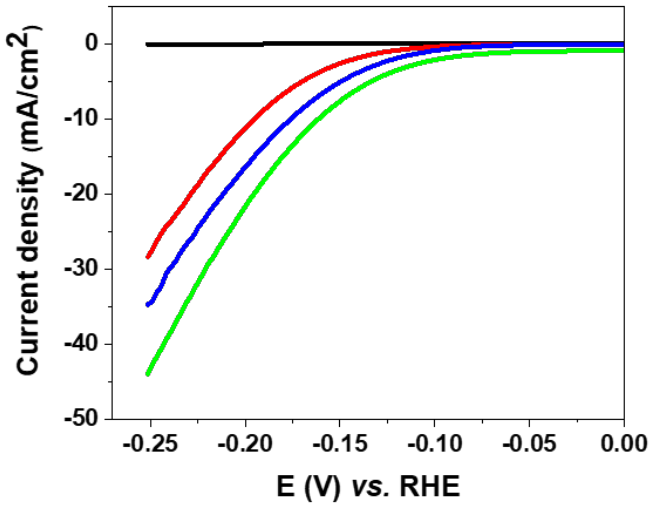

Figure S4. Steady I-V curves recorded on a 350µg-Au-NPs-13nm coated glassy carbon disk at different angular rotating rate: 0 rmp (red curve), 1000 rpm (blue curve) and 6000 (olive curve). Control I-V curve recorded on the same glassy carbon disk without Au-NPs catalyst loading is also presented (black curve). Electrolyte was a O_2-free pH 0 H_2SO_4 solution. Potential scan rate was 2 mV/s.

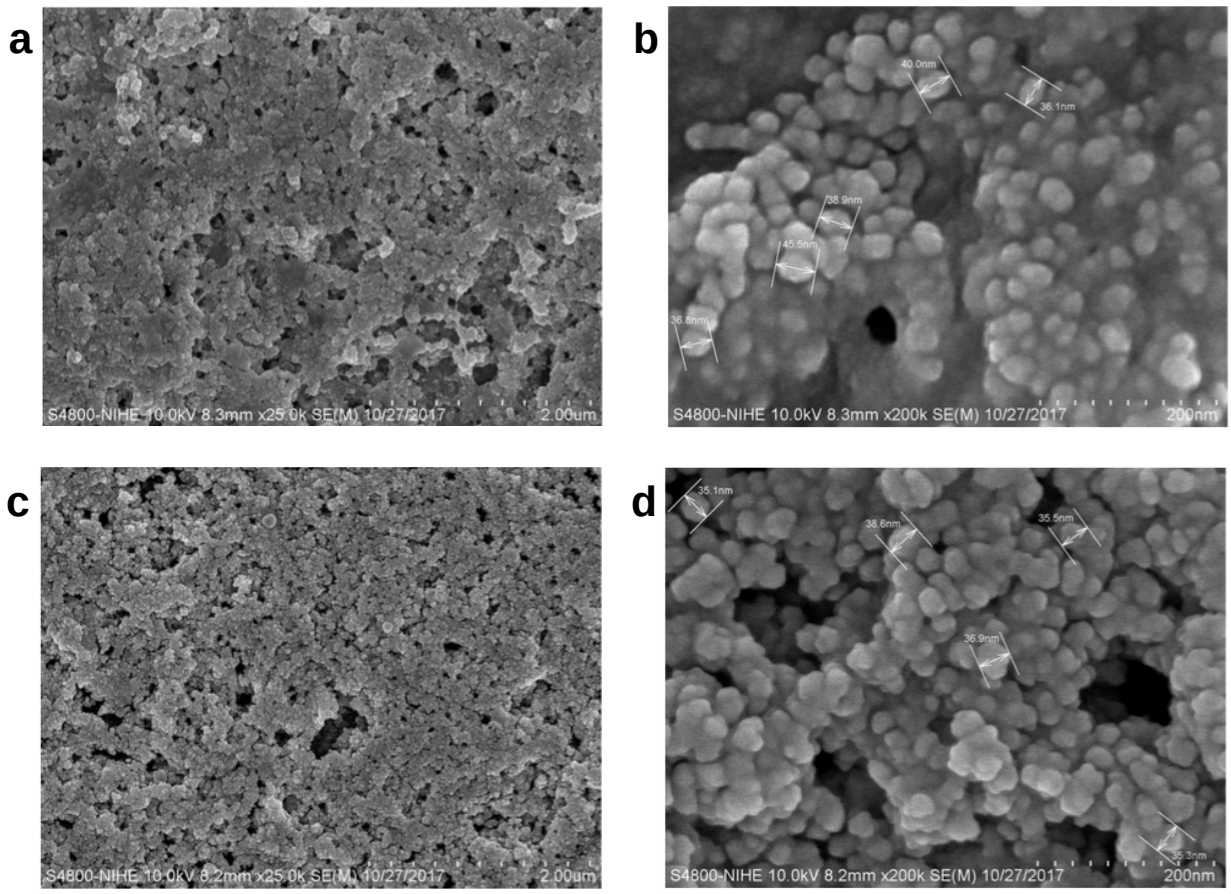

Figure S5. SEM images of the as-prepared 70μg-Au-NPs-13nm/FTO electrode (**a** and **b**) and the steady 70μg-Au-NPs-13nm/FTO electrode (**c** and **d)**.

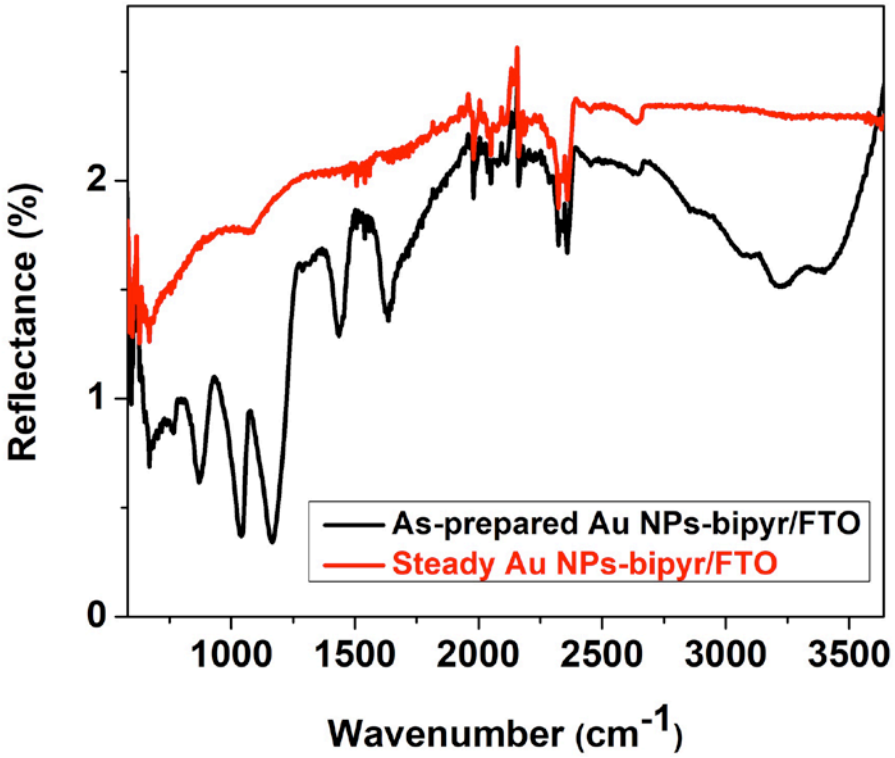

Figure S6. ATR-IR spectra of a 350µg-Au-NPs-13nm/FTO electrode immersed in a solution containing bipyridine ligand (black trace) and the same electrode after repeating the cathodic potential polarization (red trace).

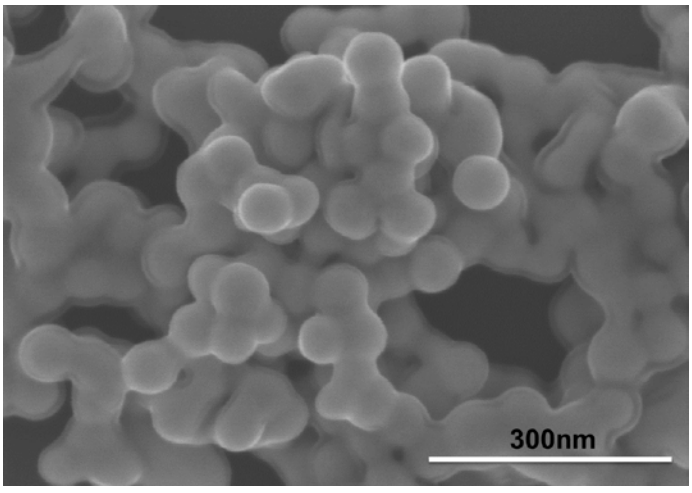

Figure S7. SEM image recorded on a 70µg-Au-NPs-60nm/FTO electrode

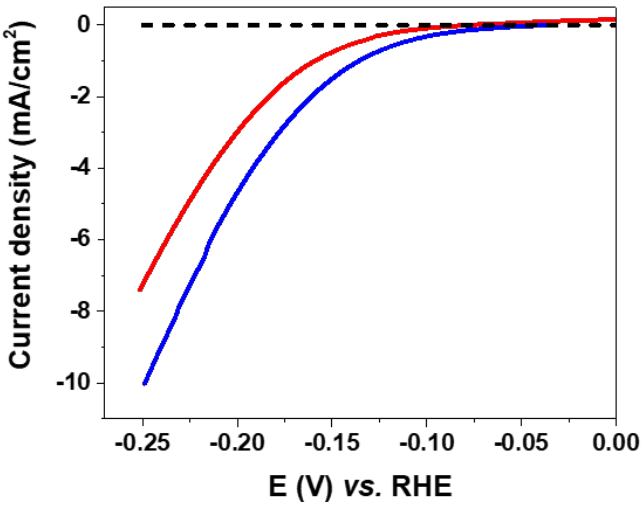

Figure S8. Steady I-V curves recorded on a 70µg-Au-NPs-13nm/FTO (blue curve) and a 70µg-Au-NPs-60nm/FTO (red curve) electrodes. Control I-V curve recorded on a clean FTO electrode without Au-NPs catalyst loading is also presented (black dashed curve). Electrolyte was a O_2-free pH0 H_2SO_4 solution. Potential scan rate was 2 mV/s.

Table S1: HER activity of some selected (best) Pt-free catalysts

Entry	Catalyst	Onset overpotential η (mV)	η (mV) at 10 mA/cm²	j (mA/cm²) at η 200mV	TOFs (s^{-1})	Tafel slope (mV/decade)	pH	Refs
1	$Ni_{43}Au_{57}$	70	160	17.5	NA	43	0	[1]
2	MoS_2/graphene	100	150	30	NA	41	0	[2]
3	Strained vacancy MoS_2	60	170	15	7.5 (η100mV)	60	0.2	[3]
4	$[Mo_3S_4]^{4+}$	150	250	5	0.07 (η 0mV)	120	0	[4]
5	MoS_2/Au NPs	230	350	-	NA	57-66	0	[5]
6	$[Mo_3S_{13}]^{2-}$/Au	150	>300	0.6	0.47 (η 200mV)	58	0	[6]
7	$[Mo_2S_{12}]^{2-}$	100	161	65	3.27 (η 200 mV)	39	0	[7]
8	$[Mo_3S_{13}]^{2-}$	100-120	180-220	5-27.5	3 (η 200mV)	38-40	0	[8]
9	MoS_2/Au(111)				10 (η 160mV)			[9]
10	Mo_2N/C/AuNP (5-8 nm)	200	300	-	NA	63	0	[10]
11	Au(111)	130	350	NA	NA	60-120		[11]
12	Au rods	280	>400	NA	NA	105	0	[12]
13	Au/MoS_2	220	320	NA	NA	86	0	[12]
14	Au NPs (10 nm)/C	99-125	>350	NA	$4.43.10^{-4}$ (η 350 mV)	76.6-100.6	0	[13]
15	Ni_2P	30	100		0.015 (η 100 mV) 0.50 (η 200 mV)	46		[14]
16	CoS_2 NW	75	145	NA	NA	51.6	0	[15]

References

1. H. Lv, Z. Xi, Z. Chen, S. Guo, Y. Yu, W. Zhu, Q. Li, X. Zhang, M. Pan, G. Lu, S. Mu and S. Sun, *J. Am. Chem. Soc.*, 2015, **137**, 5859-5862

2. Y. Li, H. Wang, L. Xie, Y. Liang, G. Hong and H. Dai, *J. Am. Chem. Soc.*, 2011, **133**, 7296-7299.

3. H. Li, C. Tsai, A. L. Koh, L. Cai, A. W. Contryman, A. H. Fragapane, J. Zhao, H. S. Han, H. C. Manoharan, F. Abild-Pedersen, J. K. Norskov and X. Zheng, *Nat. Mater.*, 2016, **15**, 48-53.

4. T. F. Jaramillo, J. Bonde, J. Zhang, B.-L. Ooi, K. Andersson, J. Ulstrup and I. Chorkendorff, *J. Phys. Chem. C.*, 2008, **112**, 17492-17498.

5. J. Kim, S. Byun, A. J. Smith, J. Yu and J. Huang, *J. Phys. Chem. Lett.*, 2013, **4**, 1227-1232.

6. T. R. Hellstern, J. Kibsgaard, C. Tsai, D. W. Palm, L. A. King, F. Abild-Pedersen and T. F. Jaramillo, *ACS Catal.*, 2017, **7**, 7126-7130.

7. Z. Huang, W. Luo, L. Ma, M. Yu, X. Ren, M. He, S. Polen, K. Click, B. Garrett, J. Lu, K. Amine, C. Hadad, W. Chen, A. Asthagiri and Y. Wu, *Angew. Chem. Int. Ed.*, 2015, **54**, 15181-15185

8. J. Kibsgaard, T. F. Jaramillo and F. Besenbacher, *Nat. Chem.*, 2014, **6**, 248

9. T. F. Jaramillo, K. P. Jorgensen, J. Bonde, J. H. Nielsen, S. Horch, Ib Chorkendorff, *Science*, 2007, **317**, 100-102

10. U. Joshi, J. Lee, C. Giordano, S. Malkhandi and B. S. Yeo, *Phys. Chem. Chem. Phys.*, 2016, **18**, 21548-21553.

11. J. Perez, E. R. Gonzalez and H. M. Villullas, *J. Phys. Chem. B*, 1998, **102**, 10931-10935.

12. Y. Shi, J. Wang, C. Wang, T.-T. Zhai, W.-J. Bao, J.-J. Xu, X.-H. Xia and H.-Y. Chen, *J. am. Chem. Soc.*, 2015, **137**, 7365-7370.

13. Y. Wang, Y. Sun, H. Liao, S. Sun, S. Li, J. W. Ager and Z. J. Xu, *Electrochimica Acta*, 2016, **209**, 440-447.

14. E. J. Popczun, J. R. McKone, C. G. Read, A. J. Biacchi, A. M. Wiltrout, N. S. Lewis and R. E. Schaak, *J. Am. Chem. Soc.*, 2013, **135**, 9267-9270.

15. M. S. Faber, R. Dziedzic, M. A. Lukowski, N. S. Kaiser, Q. Ding and S. Jin, *J. Am. Chem. Soc.*, 2014, **136**, 10053-10061.